



Demethylbellidifolin isolated from *Swertia bimaculata* against human carboxylesterase 2: Kinetics and interaction mechanism merged with docking simulations



Tian-Tian Liu^{a,1}, Xiao-Kui Huo^{a,1}, Xiang-Ge Tian^{a,1}, Jia-Hao Liang^a, Jing Yi^a, Xin-Yue Zhang^a, Song Zhang^a, Lei Feng^a, Jing Ning^a, Bao-Jing Zhang^a, Cheng-Peng Sun^{a,*}, Xiao-Chi Ma^{a,b,*}

^a College of Pharmacy, College (Institute) of Integrative Medicine, The National & Local Joint Engineering Research Center for Drug Development of Neurodegenerative Disease, Dalian Medical University, Dalian, China

^b Jiangsu Key Laboratory of New Drug Research and Clinical Pharmacy, Xuzhou Medical University, Xuzhou, China

ARTICLE INFO

Keywords:

HCE 2
Inhibitor
Molecular docking
Traditional Chinese medicines

ABSTRACT

In this study, forty-nine kinds of traditional Chinese medicines (TCMs) were evaluated for their inhibitory activities against human carboxylesterase 2 (HCE 2) using a human liver microsome (HLM) system. *Swertia bimaculata* showed significant inhibition on HCE 2 at 10 µg/mL among forty-nine kinds of TCMs. The extract of *Swertia bimaculata* was separated by preparative HPLC to afford demethylbellidifolin (1) identified by MS, ¹H NMR, and ¹³C NMR spectra. Demethylbellidifolin (1) was assayed for its inhibitory HCE 2 effect by HCE 2-mediated DDAB hydrolysis, and its potential IC₅₀ value was 3.12 ± 0.64 µM. Demethylbellidifolin (1) was assigned as a mixed-type competitive inhibitor with the inhibiton constant Ki value of 6.87 µM by Lineweaver-Burk and slope plots. Living cell imaging was conducted to corroborate its inhibitory HCE 2 activity. Molecular docking indicated potential interactions of demethylbellidifolin (1) with HCE 2 through two hydrogen bonds of the C-3 and C-5 hydroxy groups with amino acid residues Glu227 and Ser228 in the catalytic cavity, respectively.

1. Introduction

Recently, carboxylesterase 2 (CE 2) has been identified as an important modulator of safety and efficacy for oral ester-containing drugs [1–4]. CE 2 is the major isoform of human carboxylesterases in the gastrointestinal tract, and is responsible for the carboxyester hydrolysis of endogenous and exogenous substances, which makes it the main enzyme involved in intestinal first-pass metabolism [2]. Inhibition of CE 2 improved the oral bioavailability of substrate drugs [5–8]. Furthermore, CE 2-mediated local accumulation of toxic metabolites exacerbates gastrointestinal toxicity of irinotecan, a carbamate prodrug for the treatment of colorectal cancer. It was reported that CE 2 inhibitors changed the distribution of irinotecan and its toxic metabolite SN-38 in the intestine to alleviate irinotecan-induced diarrhea [8–12]. So far, some human carboxylesterase 2 (HCE 2) inhibitors have been synthesized by chemists and isolated from traditional Chinese medicine (TCM) [13–16], such as protostanes [17–20], β-lapachones [21], flavones [22–24], and abietanes [25]. Therefore, searching for new HCE 2

inhibitors from TCMs has attracted attention from chemists to increase the bioavailability of oral ester-containing drugs or alleviate the gastrointestinal toxicity of irinotecan.

In order to discover potent HCE 2 inhibitors from TCMs, forty-nine kinds of TCMs that contained triterpenoids and flavones were selected, and assayed for their inhibitory activities against HCE 2. Among them, *Swertia bimaculata* possessed significantly inhibitory activity against HCE 2, therefore, further separation of *Swertia bimaculata* led to the isolation of a novel inhibitor demethylbellidifolin (1). Inhibition kinetics and molecular docking were performed to investigate the potential mechanism between demethylbellidifolin (1) and HCE 2.

2. Results and discussion

2.1. *Swertia bimaculata* could inhibit HCE 2 activity.

HCE 2 is a critical phase I metabolic enzyme, and many potent HCE 2 inhibitors have been discovered from natural products [13–15], such

* Corresponding authors at: College of Pharmacy, Dalian Medical University, Dalian, China (C.P. Sun); Jiangsu Key Laboratory of New Drug Research and Clinical Pharmacy, Xuzhou Medical University, Xuzhou, China (X.C. Ma).

E-mail addresses: suncp146@163.com (C.-P. Sun), maxc1978@126.com (X.-C. Ma).

¹ These authors contributed equally to this work.

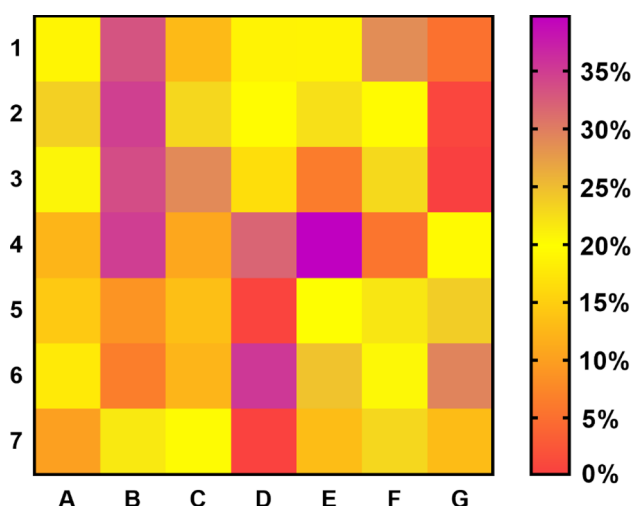


Fig. 1. The inhibitory activities of forty-nine kinds of traditional Chinese medicines against HCE 2 at 10 µg/mL. Each grid represented a TCM, and the color of each grid represented the inhibitory activity of each TCMs. Forty-nine kinds of traditional Chinese medicines were listed in Table S1.

as protostanes [17–20], beta-lapachones [21], and flavonoids [22,23], which inspired us to search for novel inhibitors from TCMs. Therefore, we screened inhibitory activities of forty-nine kinds of TCMs against HCE 2 at the concentration of 10 µg/mL through the method of HCE 2-mediated fluorescent probe substrate DDAB hydrolysis (Fig. 1 and Table S1). As shown in Fig. 1 and Table S1, seven kinds of TCM extracts could inhibit more than 30% of HCE 2 activity at a concentration of 10 µg/mL, including *Pogostemon cablin* (1B), *Sophora japonica* (2B), *Rehmannia glutinosa* (3B), *Serissa japonica* (4B), *Schizonepeta tenuisfolia* (4D), *Baphicacanthus cusia* (6D), and *Swertia bimaculata* (4E). Among them, *Swertia bimaculata* could inhibit approximately 40% activity against HCE 2 at a concentration of 10 µg/mL, and displayed the most potent inhibitory activity than any of TCMs, revealing the inhibitory potentiality of phytochemical constituents in *Swertia bimaculata* against HCE 2.

2.2. The discovery of a novel inhibitor from *Swertia bimaculata* against HCE 2

The extract of *Swertia bimaculata* was separated by preparative HPLC to yield fifteen fractions Fr.1-Fr.15, and Fr.10-Fr.15 showed substantial inhibitory activities as their inhibitory rates from 73.6% to 85.8% at 10 µg/mL (Fig. 2A). Their inhibitory effects IC₅₀ values was 3.48 ± 0.28, 1.99 ± 0.26, 0.53 ± 0.06, 0.21 ± 0.03, 0.77 ± 0.17, and 0.35 ± 0.11 µg/mL, respectively. Fr.13 possessed the most inhibitory potential; therefore, it was separated by preparative HPLC, leading to the isolation of compound 1.

Compound 1 was obtained as a light yellow powder, and it had a molecular formula of C₁₃H₈O₆ on a basis of its HRMS (*m/z* 259.0258 [M – H]⁻, calcd for C₁₃H₇O₆, 259.0243) and ¹³C NMR data. The ¹H NMR spectrum of compound 1 (Table 1) displayed signals of four aromatic protons [δ_H 7.23 (1H, d, *J* = 8.8 Hz), 6.62 (1H, d, *J* = 8.8 Hz), 6.41 (1H, d, *J* = 1.7 Hz), and 6.22 (1H, d, *J* = 1.7 Hz)]. The ¹³C NMR data of compound 1 (Table 1) showed 13 carbon signals, including one ketonic carbonyl carbon (δ_C 183.7) and twelve aromatic carbons (δ_C 166.5, 162.3, 157.4, 151.8, 143.3, 137.2, 123.6, 109.4, 107.3, 101.2, 98.4, and 94.3), suggesting that compound 1 was a xanthone-type flavonoid. The ¹H and ¹³C NMR data of compound 1 were identical with those of demethylbellidifolin [26,27], therefore, compound 1 was assigned as demethylbellidifolin (Fig. 3).

2.3. The inhibitory activity of demethylbellidifolin (1) against HCE 2.

The inhibitory activity of demethylbellidifolin (1) against HCE 2

was determined by HCE 2-mediated DDAB hydrolysis in the HLM system. Demethylbellidifolin (1) could dose-dependently inhibit HCE 2-mediated DDAB hydrolysis with IC₅₀ value of 3.12 ± 0.64 µM (Fig. 4A), and display more inhibitory activity than the positive drug loperamide (IC₅₀ = 14.82 ± 0.59 µM) as previously described [28], which encouraged us to further investigate its inhibition kinetics.

2.4. The inhibition kinetics of demethylbellidifolin (1) against HCE 2.

Demethylbellidifolin (1) displayed more potent inhibitory effect against HCE 2 than that of the positive drug loperamide, therefore, its inhibition kinetics was performed, and its inhibition type and inhibition constant (Ki) were analyzed by Michealis-Menten, Lineweaver-Burk, and slope plots (Fig. 4). As shown in Lineweaver-Burk plot (Fig. 4C), a series of lines intersected at the second quadrant, and Km and Vmax were all decreased with the increase of the inhibitor concentration, revealing that demethylbellidifolin (1) was a mixed-type competitive inhibitor, and its Ki value was 6.87 µM calculated by Slope plot (Fig. 4D).

2.5. Demethylbellidifolin (1) displayed the inhibitory activity against HCE 2 in living cell level

In order to validate the inhibitory effect of demethylbellidifolin (1) in living cell through a visual manner, human colon cancer cell LoVo was incubated with DDAB (10 µM) and Hoechst 33342 in the absence or presence of demethylbellidifolin (1). DDAB, as a substrate of HCE 2, can be hydrolyze by HCE 2 to afford DDAO that is a fluorochrome, therefore, the activity of HCE 2 in living cells can be imaged by staining DDAO. Hoechst 33342 is a blue fluorochrome of cell nucleus that can penetrate the cell membrane, and it can bind to double-stranded DNA with λ_{ex} 350 nm and λ_{em} 461 nm. Compared with the blank group, the probe DDAB could be hydrolyzed by HCE 2, and LoVo cells was stained red (Fig. 5), which indicated that DDAB could be used as a substrate of HCE 2. Demethylbellidifolin (1) could significantly inhibit the activity of HCE 2 in living cell compared with the DDAB group, which confirmed its experimental result *in vitro*.

2.6. Molecular docking

Demethylbellidifolin (1) displayed substantial inhibitory HCE 2 effect *in vitro* and in living cell level, which encouraged us to investigate the potential action mechanism between demethylbellidifolin (1) and HCE 2 by molecular docking using Discovery Studio 3.5 according to our previous method [28]. The homology structure of hCE 2 was built using the Discovery Studio program based on 3D structure of HCE 1 (PDB: 1YAH). The 3D structure of demethylbellidifolin (1) was subjected to energy minimization with the CHARMM force field parameters. The bioactive binding conformation of demethylbellidifolin (1) within HCE 2 was probed using CDOCKER. As shown in Fig. 6 and Table 2, demethylbellidifolin (1) could be docked into the ligand-binding domain (LBD) of HCE 2 with the lowest energy of -33.00 kcal/mol in Fig. 6 that showed their interactions, including hydrogen bond, carbon hydrogen bond, π-π bond, and π-σ bond. Among important interactions between ligand and protein [24,28], the hydroxy group at C-3 had an interaction with the amino acid residue Glu227 that was located in the catalytic cavity by a hydrogen bond [29], and another hydrogen bond of the hydroxy group at C-5 with the amino acid residue Ser228 that was in charge of catalysis was also observed [2,29]. This result was similar to those of the previous studies [2,23,28,29], which suggested that Glu227 and Ser228 played vital roles in the inhibition of demethylbellidifolin (1) on HCE 2. This finding indicated the potential interaction of demethylbellidifolin (1) and HCE 2, and demethylbellidifolin (1) could be regarded as a potential inhibitor of HCE 2.

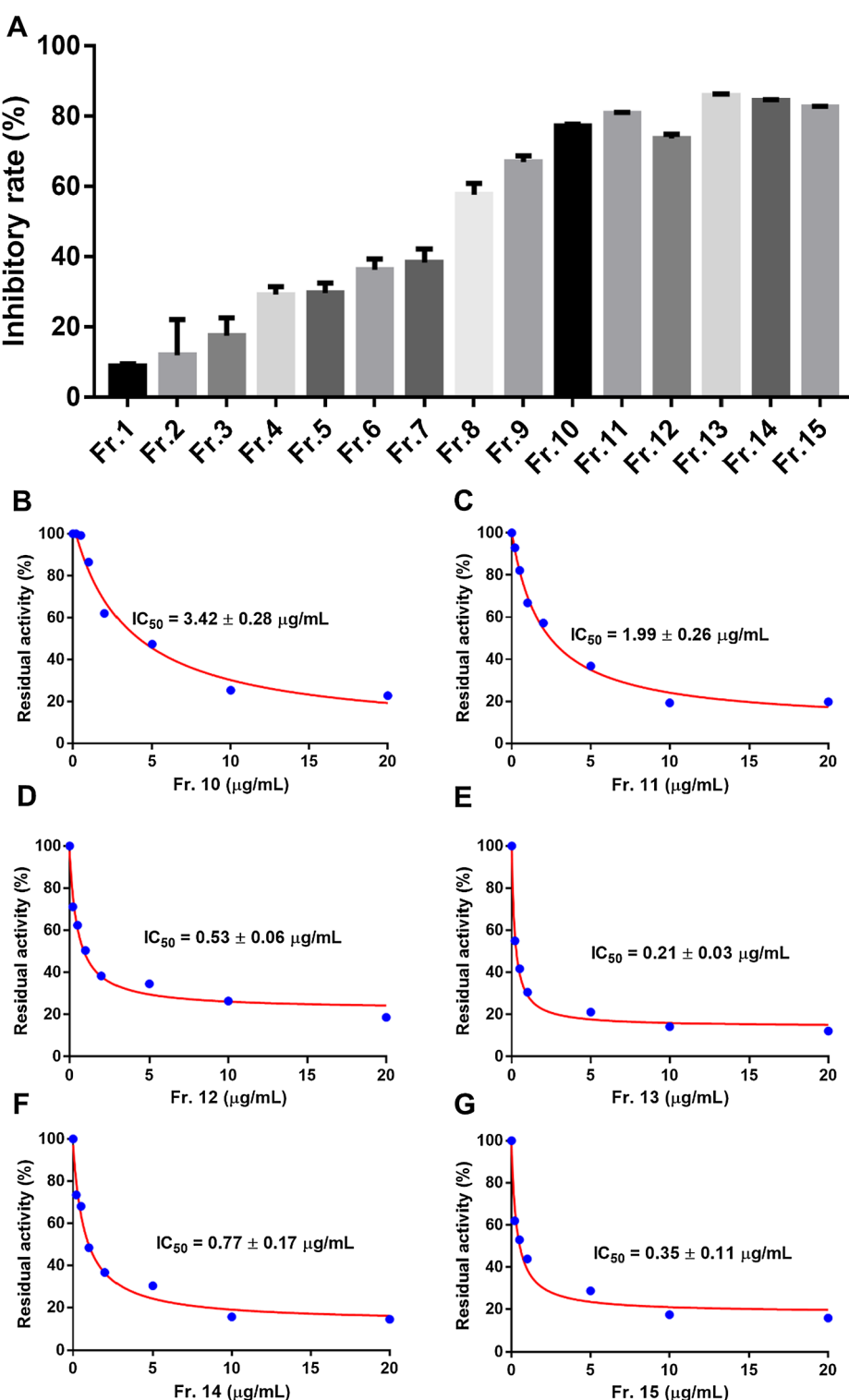


Fig. 2. (A) The inhibitory activities of fifteen fractions of extract of *Swertia bimaculata* against HCE 2 at 10 $\mu\text{g/mL}$; (B-G) Fractions 10–15 displayed dose-dependently inhibitory activities against HCE 2.

3. Conclusion

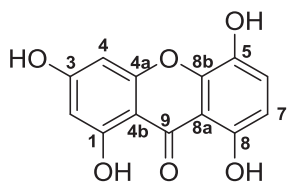
In this study, we assayed inhibitory activities of forty-nine kinds of TCMs against HCE 2. *Swertia bimaculata* showed significantly inhibitory activity against HCE 2 at 10 $\mu\text{g/mL}$ in forty-nine kinds of TCMs, and separation of *Swertia bimaculata* resulted in the isolation of a novel inhibitor demethylbellidifolin (1) with IC_{50} value of $3.12 \pm 0.64 \mu\text{M}$.

According to the inhibition kinetics result, its K_i value was $6.87 \mu\text{M}$ as a mixed-type competitive inhibitor. Its inhibitory activity against HCE 2 was confirmed in the living cell level. Molecular docking was performed to investigate the interaction between demethylbellidifolin (1) and HCE 2, indicating the presence of two hydrogen bonds between the hydroxy group at C-3 and the amino acid residue Glu227 in the catalytic cavity, and the hydroxy group at C-5 and the amino acid residue Ser228 that

Table 1

^1H (600 MHz) and ^{13}C NMR (150 MHz) data of demethylbellidifolin (1) in DMSO- d_6 .

No.	δ_{C}	δ_{H} (J in Hz)	No.	δ_{C}	δ_{H} (J in Hz)
1	162.2		6	123.6	7.23, d (8.8)
2	98.4	6.22, d (1.7)	7	109.4	6.62, d (8.8)
3	166.5		8	151.8	
4	94.3	6.41, d (1.7)	8a	107.3	
4a	157.4		8b	101.2	
4b	143.3		9	183.7	
5	137.2				

**Fig. 3.** The structure of demethylbellidifolin (1) from *Swertia bimaculata*.

was in charge of catalysis. This result suggested that demethylbellidifolin (1) could be regarded as a leading compound to develop novel HCE 2 inhibitors.

4. Material and methods

4.1. General experimental procedures

Forty-nine kinds of TCMs, *Akebia quinata* (Thunb.) Decne, *Pogostemon cablin* (Blanco) Benth., *Raphanus sativus* L., *Glycine max* (L.) Merr., *Coix lacryma-jobi* L. var. ma-yuen (Roman.) Stapf., *Cinnamomum cassia* Presl., *Dipsacus asperoides* C. Y. Cheng et T. M. Ai, *Trachelospermum jasminoides* (Lindl.) Lem., *Sophora japonica* L., *Trichosanthes kirikwii* Maxim., *Corydalis bungeana* Turcz., *Prunus mume* (Sieb.) Seib. et Zucc., *Scutellaria barbata* Don., *Phragmites communis* Trin., *Boehmeria nivea* (L.) Gaud., *Rehmannia glutinosa* (Gaetn.) Libosch.

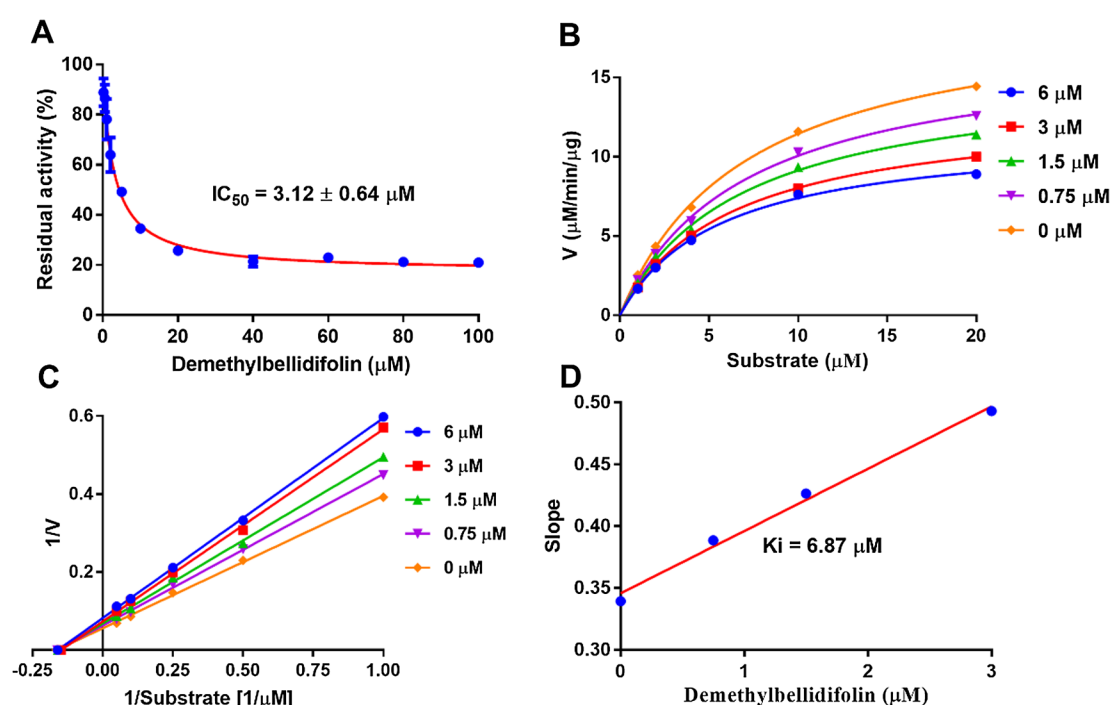
ex Fisch. et Mey., *Polygonum cuspidatum* Sieb. et Zucc., *Citrus grandis* Osbeck var. *tomentosa* Hort., *Cinnamomum cassia* Presl., *Prinsepia uniflora* Batal, *Ziziphus jujuba* Mill. var. *spinosa* (Bunge) Huex H. F. Chou, *Liquidambar formosana* Hance, *Serissa japonica* (Thunb.) Thunb., *Bambusa textilis* Mc Clure, *Schizonepeta tenuifolia* Briq., *Hedyotis diffusa* Wall., *Selaginella doederleinii* Hieron., *Spatholobus suberectus* Dunn., *Allium tuberosum* Rott ex Spreng., *Potentilla discolor* Bge., *Dendranthema morifolium* (Ramat.) Tzvel., *Swertia bimaculata* (Sieb. et Zucc.) Hook. Thoms. ex Clarke, *Phellodendron chinense* Schneid., *Spirodela polyrrhiza* (L.) Schleid., *Artemisia argyi* Lev. et Vant., *Aralia chinensis* L., *Cirsium japonicum* Fisch. ex DC., *Ailanthus altissima* (Mill.) Swingle, *Baphicacanthus cusia* (Nees) Bremek., *Dendranthema indicum* (L.) Des Moul. (Compositae), *Belamcanda chinensis* (L.) Redouté, *Dioscorea septemloba* Thunb., *Eucommia ulmoides* Oliv., *Siphonostegia chinensis* Benth., *Nelumbo nucifera* Gaertn., *Polygonum aviculare* L., *Campsis grandiflora* (Thunb.) K. Schum., *Piper longum* L., and *Piper puberulum* (Benth.) Maxim., were purchased from Beijing Tongren Tang, China. Human liver microsome (HLM) was purchased from Research Institute of Liver Diseases Co., Ltd. (Shanghai, China).

4.2. Preparation of forty-nine kinds of TCM extracts

Each of TCMs (20 g) was extracted by 95% EtOH (v/v) for 2 h, and the extract was concentrated at 45 °C *in vacuo* to afford the residue. Then, the residue (10 mg) was dissolved in DMSO (1 mL), and stored at 4 °C.

4.3. Extraction and isolation

Swertia bimaculata (200 g) was extracted by 95% EtOH (5 L) for 2 h and three times. The extract was separated by preparative HPLC eluted with MeOH-H₂O (from 10% to 90%, v/v), resulting in the isolation of fifteen fractions (Fr.1-Fr.15). Finally, compound 1 (2.3 mg) was isolated from Fr.13 through preparative HPLC eluted with 60% MeOH.

**Fig. 4.** (A) Demethylbellidifolin (1) dose-dependently inhibited HCE 2 activity. (B) Michealis-Menten plot of demethylbellidifolin (1) against HCE 2. (C) Lineweaver-Burk plot of demethylbellidifolin (1) against HCE 2. (D) Slope plot of demethylbellidifolin (1) against HCE 2.

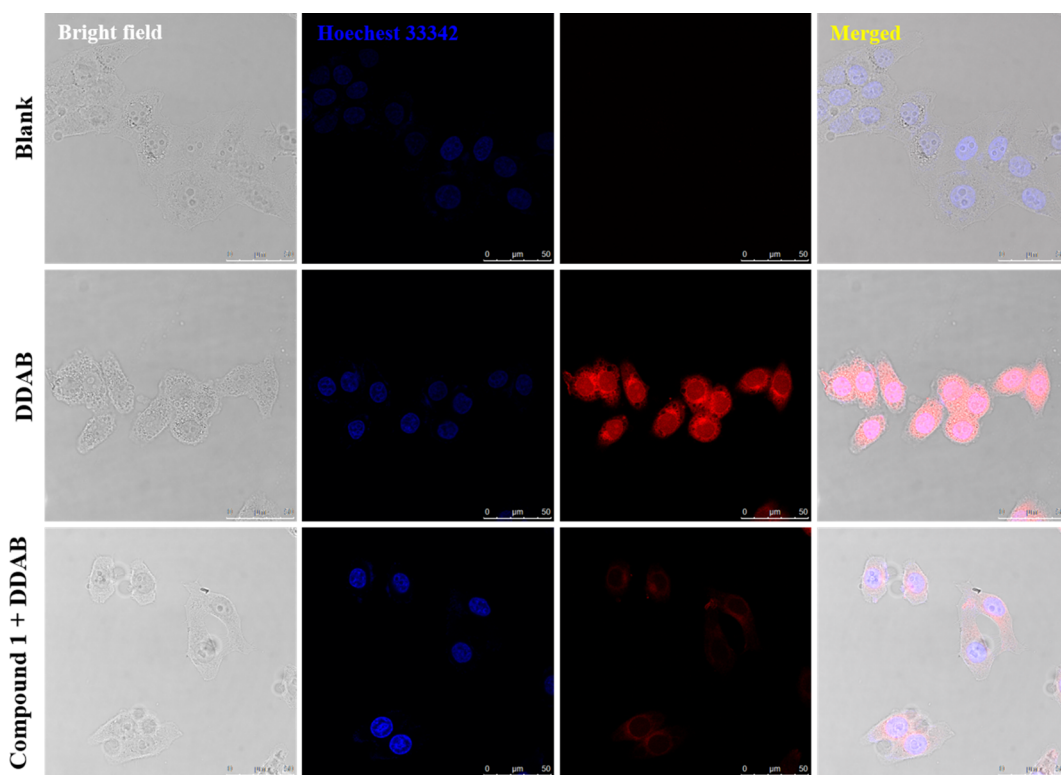


Fig. 5. Demethylbellidifolin (**1**) displayed significantly inhibitory activity against HCE 2 at 10 μ M in living cell level ($\lambda_{\text{ex}} = 633 \text{ nm}$, $\lambda_{\text{em}} = 640\text{--}690 \text{ nm}$). Human colon cancer cell LoVo was incubated with DDAB (10 μ M, red) or Hoechst 33342 (blue) in the absence or presence of demethylbellidifolin (**1**, 10 μ M).

4.4. HCE 2 bioassay

Forty-nine kinds of TCMs and compound **1** were assayed for their inhibitory activities against HCE 2 based on HCE 2-mediated the substrate 7-benzoyl-1,3-dichloro-9,9-dimethyl-9*H*-acridin-2-one (DDAB) hydrolysis in the HLM system as our previous described [30], respectively. Loperamide was regarded as a positive drug [26]. Forty-nine kinds of TCM extracts (10 μ g/mL) or compound **1** (from 0.1 μ M to 100 μ M) were incubated with HLM (0.04 mg/mL) and probe DDAB (10 μ M) in potassium phosphate buffer (pH 7.4, 100 mM) at 37 °C for 30 min. Then, the fluorescence signals were recorded on a microplate reader using excitation wavelength of 600 nm.

4.5. Inhibitory kinetic analysis

The inhibitory behavior of compound **1** was evaluated using substrate DDAB according to our previous methods [31–33]. Line-weaver–Burk and slope plots were performed to define whether the inhibition was competitive, noncompetitive, uncompetitive, or mixed-type inhibition, and calculate the inhibition constant K_i value.

4.6. Living cell imaging

LoVo cells were cultivated in RPMI-1640 medium (10% fetal bovine serum, FBS) in the atmosphere with 5% CO₂ at 37 °C. 1×10^5 of Cells/well were seeded in 6-well plate, and incubated for a night [34,35]. Cells were pre-treated with or without compound **1** (10 μ M) for 1 h, and then treated with or without Hoechst 33342 and DDAB (10 μ M) at 37 °C for 30 min. Finally, cells were imaged on a Leica TCS SP8 confocal microscope.

4.7. Molecular docking

A sequence similarity search was performed to identify the template

(HCE **1**) with sequence similarity 48.24%. The homology HCE 2 structure was constructed on a basis of the HCE 1 crystal structure (PDB ID: [1YAH](#)) and the information of amino acid sequence of HCE 2 (amino acid sequence: O00748) using Discovery Studio 3.5 (Accelrys, SanDiego, CA, USA) according to previously described [29]. The model of HCE 2 was optimized through a 25 ns dynamic calculation by AMBER 10 [36]. And the optimized model was further evaluated by Pro-check server which is used to check the stereochemical quality of a protein structure by analyzing residue-by-residue geometry and overall structure geometry [37]. The results showed that Residues in disallowed regions was just 0.6%, indicating that the model is acceptable for further docking. The CDOCKER protocol was used to perform molecular docking. The binding site was defined according to similar substrate binding to the area in HCE 1 covered by a radius of 9.5 Å. The preparation of protein structure, including adding hydrogen atoms, removing water molecules, and assigning Charmm forcefield. Goldscore was selected as the score function. A maximum of 20 conformations was generated. The maximum number of poses per ligand was set to 30 with a minimum RMSD between final poses of 0.50 Å. The kinetic optimization temperature is 1000 °C, the optimization steps are 10,000 steps. The non-bond interaction is calculated based on the lattice technique, and the other parameters are the default values of the system.

4.8. Statistical analysis

The statistical analysis was performed with GraphPad Prism 7.0 for Windows. All data are presented as means \pm SD.

Declaration of Competing Interest

The authors declare no competing financial interest.

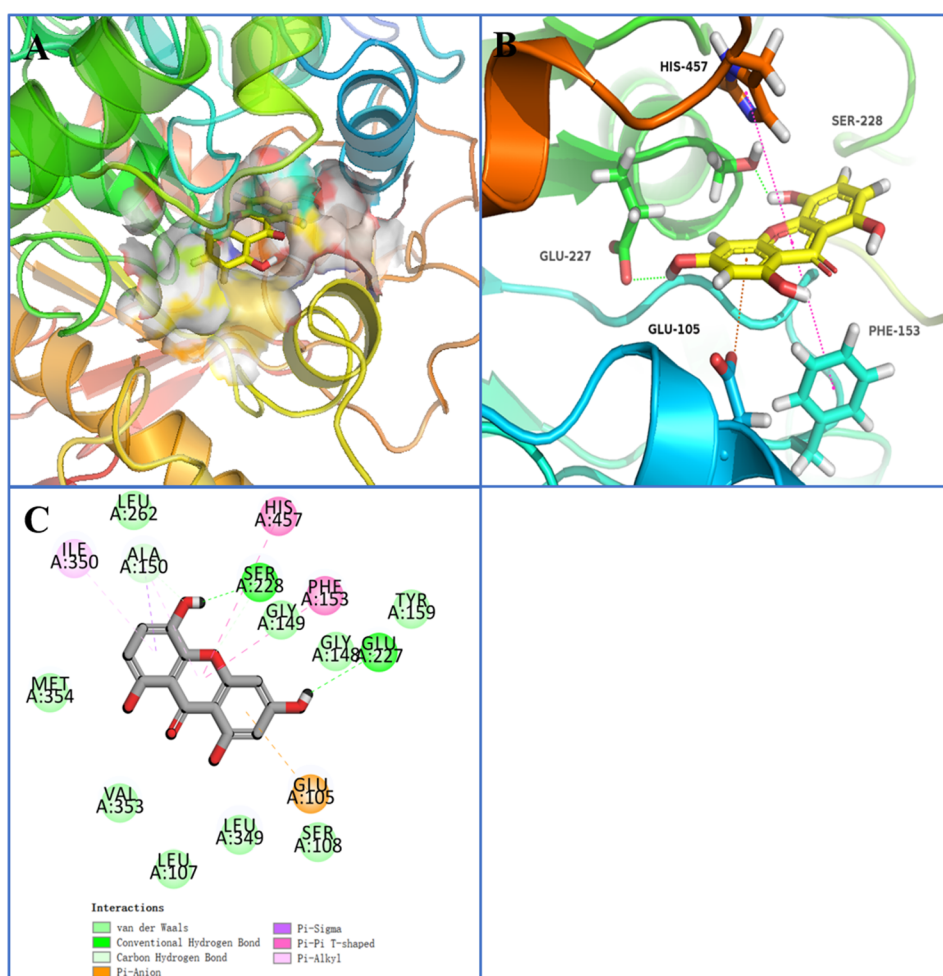


Fig. 6. (A) Demethylbellidifolin (1) could be bonded to LBD of HCE 2. (B) 3D structures of demethylbellidifolin (1) with HCE 2. (C) 2D interactions between demethylbellidifolin (1) and HCE 2.

Table 2
Interaction information of demethylbellidifolin (1) with HCE 2.

Compound	Interaction amino acids	Hydrogen bonds	Binding Energy (kcal/mol)
1	Glu105, Ala150, Phe153, Glu227, Ser228, Ile350, His457	Glu227, Ser228	-33.00

Acknowledgments

This work was supported by National Natural Science Foundation of China (No. 81703679), National Key Research and Development Program of China (No. 2018YFC1705900), Distinguished Professor of Liaoning Province program, and the Liaoning Revitalization Talents Program.

Appendix A. Supplementary material

Supplementary data to this article can be found online at <https://doi.org/10.1016/j.bioorg.2019.103101>.

References

- [1] T. Satoh, M. Hosokawa, The mammalian carboxylesterases: from molecules to functions, *Annu. Rev. Pharmacol. Toxicol.* 38 (1998) 257–288.
- [2] L.W. Zou, Y.G. Li, P. Wang, K. Zhou, J. Hou, Q. Jin, D.C. Hao, G.B. Ge, L. Yang, Design, synthesis, and structure-activity relationship study of glycyrrhetic acid
- [3] S. Bencharit, C.C. Edwards, C.L. Morton, E.L. Howard-Williams, P. Kuhn, P.M. Potter, M.R. Redinbo, Multisite promiscuity in the processing of endogenous substrates by human carboxylesterase 1, *J. Mol. Biol.* 363 (1) (2006) 201–214.
- [4] O. Soares da Silva, R. Lira de Oliveira, J. de Carvalho Silva, A. Converti, T. Souza Porto, Thermodynamic investigation of an alkaline protease from *Aspergillus tamarii* URM4634: a comparative approach between crude extract and purified enzyme, *Int. J. Biol. Macromol.* 109 (2018) 1039–1044.
- [5] T. Imai, K. Ohura, The role of intestinal carboxylesterase in the oral absorption of prodrugs, *Curr. Drug Metab.* 11 (9) (2010) 793–805.
- [6] Y. Lu, N. Bao, G. Borjihan, Y. Ma, M. Hu, C. Yu, S. Li, J. Jia, D. Yang, Y. Wang, Contribution of carboxylesterase in hamster to the intestinal first-pass loss and low bioavailability of ethyl piperate, an effective lipid-lowering drug candidate, *Drug Metab. Dispos.* 39 (5) (2011) 796–802.
- [7] K. Masaki, M. Hashimoto, T. Imai, Intestinal first-pass metabolism via carboxylesterase in rat jejunum and ileum, *Drug Metab. Dispos.* 35 (7) (2007) 1089–1095.
- [8] R. Moreira da Silva, S. Verjee, C.M. de Gaitani, A.R. Moraes de Oliveira, P.C. Pires Bueno, A.J. Cavalheiro, N. Peporine Lopes, V. Butterweck, Evaluation of the intestinal absorption mechanism of casearin X in Caco-2 cells with modified carboxylesterase activity, *J. Nat. Prod.* 79 (4) (2016) 1084–1090.
- [9] H.Y. Guan, P.F. Li, X.M. Wang, J.J. Yue, Y. He, X.M. Luo, M.F. Su, S.G. Liao, Y. Shi, Shengjiang Xiexin Decoction alters pharmacokinetics of irinotecan by regulating metabolic enzymes and transporters: a multi-target therapy for alleviating the gastrointestinal toxicity, *Front Pharmacol* 8 (2017) 769.
- [10] S.A. Huisman, W. Bijman-Lagcher, I.J. JN, R. Smits, R.W. de Bruin, Fasting protects against the side effects of irinotecan but preserves its anti-tumor effect in Apc15lox mutant mice, *Cell Cycle* 14 (14) (2015) 2333–2339.
- [11] S.A. Huisman, P. de Brujin, I.M. Ghobadi Moghaddam-Helmantel, I.J. JN, E.A. Wiemer, R.H. Mathijssen, R.W. de Bruin, Fasting protects against the side effects of irinotecan treatment but does not affect anti-tumour activity in mice, *Br. J. Pharmacol.* 173 (5) (2016) 804–814.
- [12] R.M. Wadkins, J.L. Hyatt, K.J. Yoon, C.L. Morton, R.E. Lee, K. Damodaran, P. Beroza, M.K. Danics, P.M. Potter, Discovery of novel selective inhibitors of human intestinal carboxylesterase for the amelioration of irinotecan-induced diarrhea:

- synthesis, quantitative structure-activity relationship analysis, and biological activity, Mol. Pharmacol. 65 (6) (2004) 1336–1343.
- [13] P. Stocker, M. Yousfi, O. Djerridane, J. Perrier, R. Amziani, S. El Boustani, A. Moulin, Effect of flavonoids from various Mediterranean plants on enzymatic activity of intestinal carboxylesterase, Biochimie 86 (12) (2004) 919–925.
- [14] A. Djerridane, J.M. Brunel, N. Vidal, M. Yousfi, E.H. Ajandouz, P. Stocker, Inhibition of porcine liver carboxylesterase by a new flavone glucoside isolated from *Deverra scoparia*, Chem.-Biol. Interact. 172 (1) (2008) 22–26.
- [15] A. Djerridane, M. Yousfi, B. Nadjemi, S. Maamri, F. Djireb, P. Stocker, Phenolic extracts from various Algerian plants as strong inhibitors of porcine liver carboxylesterase, J. Enzyme Inhib. Med. Chem. 21 (6) (2006) 719–726.
- [16] C. Wang, X.K. Huo, Z.L. Luan, F. Cao, X.G. Tian, X.Y. Zhao, C.P. Sun, L. Feng, J. Ning, B.J. Zhang, X.C. Ma, Alismanin A, a triterpenoid with a C₃₄ skeleton from *Alisma orientale* as a natural agonist of human pregnane X receptor, Org. Lett. 19 (20) (2017) 5645–5648.
- [17] Z.J. Zhang, X.K. Huo, X.G. Tian, L. Feng, J. Ning, X.Y. Zhao, C.P. Sun, C. Wang, S. Deng, B.J. Zhang, H.L. Zhang, Y. Liu, Novel protostane-type triterpenoids with inhibitory human carboxylesterase 2 activities, Rsc Adv. 7 (46) (2017) 28702–28710.
- [18] D. Wang, L. Zou, Q. Jin, J. Hou, G. Ge, L. Yang, Human carboxylesterases: a comprehensive review, Acta. Pharm. Sin. B 8 (5) (2018) 699–712.
- [19] L.W. Zou, T.Y. Dou, P. Wang, W. Lei, Z.M. Weng, J. Hou, D.D. Wang, Y.M. Fan, W.D. Zhang, G.B. Ge, L. Yang, Structure-activity relationships of pentacyclic triterpenoids as potent and selective inhibitors against human carboxylesterase 1, Front. Pharmacol. 8 (2017) 435.
- [20] X.L. Xin, X.Y. Zhao, X.K. Huo, X.G. Tian, C.P. Sun, H.L. Zhang, Y. Tian, Y. Liu, X. Wang, Two new protostane-type triterpenoids from *Alisma orientalis*, Nat. Prod. Res. 32 (2018) 189–194.
- [21] M.J. Hatfield, J.W. Chen, E.M. Fratt, L.Y. Chi, J.C. Bollinger, R.J. Binder, J. Bowling, J.L. Hyatt, J. Scarborough, C. Jeffries, P.M. Potter, Selective inhibitors of human liver carboxylesterase based on a beta-lapachone scaffold: Novel reagents for reaction profiling, J. Med. Chem. 60 (4) (2017) 1568–1579.
- [22] Y.Q. Wang, Z.M. Weng, T.Y. Dou, J. Hou, D.D. Wang, L.L. Ding, L.W. Zou, Y. Yu, J. Chen, H. Tang, G.B. Ge, Nevadensin is a naturally occurring selective inhibitor of human carboxylesterase 1, Int. J. Biol. Macromol. 120 (2018) 1944–1954.
- [23] Z.M. Weng, G.B. Ge, T.Y. Dou, P. Wang, P.K. Liu, X.H. Tian, N. Qiao, Y. Yu, L.W. Zou, Q. Zhou, W.D. Zhang, J. Hou, Characterization and structure-activity relationship studies of flavonoids as inhibitors against human carboxylesterase 2, Bioorg. Chem. 77 (2018) 320–329.
- [24] S.S. Song, C.P. Sun, J.J. Zhou, L. Chu, Flavonoids as human carboxylesterase 2 inhibitors: inhibition potentials and molecular docking simulations, Int. J. Biol. Macromol. 131 (2019) 201–208.
- [25] R.J. Binder, M.J. Hatfield, L.Y. Chi, P.M. Potter, Facile synthesis of 1,2-dione-containing abietane analogues for the generation of human carboxylesterase inhibitors, Eur. J. Med. Chem. 149 (2018) 79–89.
- [26] B. Lima, M. Sanchez, L. Luna, M.B. Aguero, S. Zacchino, E. Philippa, J.A. Palermo, A. Tapia, G.E. Feresin, Antimicrobial and antioxidant activities of *Gentianella multicaulis* collected on the Andean Slopes of San Juan Province, Argentina, Z. Naturforsch. C 67 (1–2) (2012) 29–38.
- [27] W. Zheng, Y.D. Yue, Y.J. Gong, Q.X. Min, Z.X. Liu, J.C. Chen, Chemical constituents of *Swertia bimaculata*, Chin. Tradition. Herbal Drugs 47 (2016) 1468–1476.
- [28] J. Yi, R. Bai, Y. An, T.T. Liu, J.H. Liang, X.G. Tian, X.K. Huo, L. Feng, J. Ning, C.P. Sun, X.C. Ma, H.L. Zhang, A natural inhibitor from *Alisma orientale* against human carboxylesterase 2: kinetics, circular dichroism spectroscopic analysis, and docking simulation, Int. J. Biol. Macromol. 133 (2019) 184–189.
- [29] G. Vistoli, A. Pedretti, A. Mazzolari, B. Testa, Homology modeling and metabolism prediction of human carboxylesterase-2 using docking analyses by Gridock: a parallelized tool based on AutoDock 4.0, J. Comput. Aid. Mol. Des. 24 (9) (2010) 771–787.
- [30] L. Feng, Y. Yang, X. Huo, X. Tian, Y. Feng, H. Yuan, L. Zhao, C. Wang, P. Chu, F. Long, W. Wang, X. Ma, Highly selective NIR probe for intestinal beta-glucuronidase and high-throughput screening inhibitors to therapy intestinal damage, ACS Sens. 3 (9) (2018) 1727–1734.
- [31] Y.L. Wang, P.P. Dong, J.H. Liang, N. Li, C.P. Sun, X.G. Tian, X.K. Huo, B.J. Zhang, X.C. Ma, C.Z. Lv, Phytochemical constituents from *Uncaria rhynchophylla* in human carboxylesterase 2 inhibition: Kinetics and interaction mechanism merged with docking simulations, Phytomedicine 51 (2018) 120–127.
- [32] H.Y. Ma, D.X. Sun, Y.F. Cao, C.Z. Ai, Y.Q. Qu, C.M. Hu, C. Jiang, P.P. Dong, X.Y. Sun, M. Hong, N. Tanaka, F.J. Gonzalez, X.C. Ma, Z.Z. Fang, Herb-drug interaction prediction based on the high specific inhibition of andrographolide derivatives towards UDP-glucuronosyltransferase (UGT) 2B7, Toxicol. Appl. Pharmacol. 277 (1) (2014) 86–94.
- [33] Z.P. Mai, K. Zhou, G.B. Ge, C. Wang, X.K. Huo, P.P. Dong, S. Deng, B.J. Zhang, H.L. Zhang, S.S. Huang, X.C. Ma, Protostane triterpenoids from the rhizome of *Alisma orientale* exhibit inhibitory effects on human carboxylesterase 2, J. Nat. Prod. 78 (10) (2015) 2372–2380.
- [34] Y. Inoue, C. Miki, H. Watanabe, J. Hiro, Y. Toiyama, E. Ojima, H. Yanagi, M. Kusunoki, Schedule-dependent cytotoxicity of 5-fluorouracil and irinotecan in a colon cancer cell line, J. Gastroenterol. 41 (12) (2006) 1149–1157.
- [35] S. Guichard, D. Cussac, I. Hennebelle, R. Bugat, P. Canal, Sequence-dependent activity of the irinotecan-5FU combination in human colon-cancer model HT-29 in vitro and in vivo, Int. J. Cancer 73 (5) (1997) 729–734.
- [36] D.A. Case, T.E. Cheatham 3rd, T. Darden, H. Gohlke, R. Luo, K.M. Merz Jr., A. Onufriev, C. Simmerling, B. Wang, R.J. Woods, The amber biomolecular simulation programs, J. Comput. Chem. 26 (16) (2005) 1668–1688.
- [37] R.A. Laskowski, M.W. MacArthur, D.S. Moss, J.M. Thornton, PROCHECK - a program to check the stereochemical quality of protein structures, J. App. Cryst. 26 (1993) 283–291.